OL 97-03

Reprinted from

PHYSICS LETTERS A

Physics Letters A 227 (1997) 340–348

Probability density function of concentration increments in a surface plume dispersing in the atmospheric boundary layer

Eugene Yee, R. Chan

Defence Research Establishment Suffield, P.O. Box 4000, Medicine Hat, Alberta, Canada T1A 8K6

Received 24 June 1996; revised manuscript received 2 December 1996; accepted for publication 31 December 1996
Communicated by C.R. Doering

N·H
ELSEVIER

24 March 1997

ELSEVIER

PHYSICS LETTERS A

Physics Letters A 227 (1997) 340–348

Probability density function of concentration increments in a surface plume dispersing in the atmospheric boundary layer

Eugene Yee, R. Chan

Defence Research Establishment Suffield, P.O. Box 4000, Medicine Hat, Alberta, Canada T1A 8K6

Received 24 June 1996; revised manuscript received 2 December 1996; accepted for publication 31 December 1996
Communicated by C.R. Doering

Abstract

The probability density function (PDF) of passive scalar concentration increments, $\Delta\Psi(r)$, across scales r in the inertial-convective subrange has been measured for a plume dispersing in the atmospheric surface layer at a large Taylor microscale based Reynolds number $R_\lambda \approx 5200$. The PDF possesses a characteristic non-Gaussian form with extended exponential tails that increase with decreasing scale. For moderately large $|\Delta\Psi(r)|$, the PDF scales in accordance to a stretched exponential form $P(\Delta\Psi) \sim \exp(-\kappa(r)|\Delta\Psi|^{q(r)})$, with a tail slope $q(r)$ (stretching exponent) and tail intercept $\kappa(r)$ (logarithmic decrement) that monotonically increases and decreases, respectively, for increasing scales r within the inertial-convective subrange. Both $q(r)$ and $\kappa(r)$ are found to be well-characterized using power-law relationships in r (viz., $q(r) \sim r^a$ and $\kappa(r) \sim r^b$), and the power-law exponents a and b in these two relationships have been empirically determined from the data. Measurements of skewness and kurtosis of the concentration increments have been obtained for a wide range of scales r. Finally, the empirical model for the behavior of the concentration increment PDF tails has been applied to extract the scaling exponents, ξ_n, associated with the moments of $\Delta\Psi(r)$ up to order 12 (i.e., the concentration structure function scaling exponents defined by the scaling law $\langle|\Delta\Psi(r)|^n\rangle \sim r^{\xi_n}$).

One of the most interesting facets of the passive scalar concentration field as it is dispersed in a turbulent flow and randomized through advection by the fluid is the scale-dependent intermittency effects in the distribution of scalar concentration. Over the past 15 years, a large amount of data has been obtained on the statistical properties of the fluctuating concentration in a turbulent plume (e.g., mean concentration, various higher-order moments such as fluctuation intensity, skewness, kurtosis, etc.) in both laboratory [1] and full-scale atmospheric field studies [2–5]. However, these studies have focussed primarily on the gross statistical description of the plume concentration and did not attempt to characterize the statistical properties of internal plume intermittency that reflect the organization of the plume concentration structure on the small scales. Statistical properties of this organization (i.e., the small-scale intermittency) have usually been characterized by the scaling behavior of the nth order structure function of concentration differences, $S_n(r) \equiv \langle|\Delta\Psi(r)|^n\rangle$, where Ψ is the instantaneous concentration, $\Delta\Psi(r) \equiv \Psi(x+r) - \Psi(x)$ is the concentration increment between two points at distance r in the direction x

PII S0375-9601(97)00031-5

of the mean velocity, and $\langle \cdots \rangle$ denotes an ensemble average.

The first step towards a physical understanding of the scaling of passive scalar concentrations was undertaken by Obukhov [6] and Corrsin [7] who extended the hypotheses of Kolmogorov's universal equilibrium theory [8] for the velocity field to the concentration field. The Obukhov–Corrsin theory for a passive scalar injected into a turbulent flow predicts that the scalar structure function obeys the following scaling law: $S_n(r) \sim r^{\xi_n}$, with $\xi_n = n/3$ in a range of r values corresponding to the inertial-convective subrange (i.e., in a range of scales smaller than those which contain most of the concentration variance and larger than those which are directly affected by molecular diffusion). For $n = 2$, the Obukhov–Corrsin prediction yields the famous 2/3 law for the averaged concentration variance fluctuations $\langle (\Delta\Psi(r))^2 \rangle$. However, careful measurements by Antonia et al. [9] have revealed that the scaling exponent ξ_n is a non-linear function of n and, hence, deviates from the predictions of the Obukhov–Corrsin theory. This deviation (anomalous scaling) arises directly from the existence of the internal intermittency caused by the organization of the fine-scale structure in the scalar concentration field. Although much experimental and theoretical effort have been expended on the characterization of the behavior of the scaling exponents ξ_n and their concomitant intermittency effects, the fundamental physics and the physical mechanisms associated with this scaling behavior is, nevertheless, currently not well understood.

In this Letter, we study the manifestation of the small-scale intermittency effects as revealed through the scale dependence of the probability density function (PDF) of the concentration increment, $\Delta\Psi(r)$, between two points separated by a distance r, using plume concentration data obtained from a tracer dispersion experiment designed to study concentration fluctuations in the atmospheric surface layer. We note that the PDF of $\Delta\Psi(r)$ provides a more complete characterization of the small-scale intermittency effect than that obtained by studying a finite number of moments of $\Delta\Psi(r)$. In this context, we measure and quantitatively characterize the shape of the PDF of $\Delta\Psi(r)$, with a particular emphasis on its tails, for a large range of separation distances r spanning the inertial-convective subrange of a scalar released into a very high Reynolds number turbulent flow (e.g., a turbulent plume dispersing in the atmospheric surface layer).

The instantaneous plume concentration data used in this study were collected near Tower Grid on U.S. Army Dugway Proving Ground, Utah (40°06′ N, 112°59′ W), about 2 km west of Camel Back Ridge on the edge of the Great Salt Lake Desert, during the fourth intensive field campaign of the cooperative Concentration Fluctuation Experiments (CONFLUX) project. These field experiments are described in detail in Yee et al. [10] and, in consequence, we include here only a brief description of the essential information. During May, 1994, when the data were collected, the field experimental site was uniform and homogeneous, covered with short grass interspersed with a few low shrubs that are less than 0.5 m in height, providing an upwind fetch that is absolutely uniform and unobstructed for 5 km or more in the direction of the prevailing winds. Measurements were made of the instantaneous plume concentration at a height of 3 m above ground level on the lateral mean-plume centerline at a distance of 50 m downwind from a continuously emitting point source deployed at a release height of 1 m above ground. Propylene (C_3H_6), which has a Schmidt number ($\equiv \nu/D$, where ν is the kinematic viscosity of air and D is the molecular diffusivity of propylene in air) of about 1, was used as the tracer gas. Hence, the conduction cutoff scale (i.e., Batchelor scale) at which molecular diffusion becomes important in the concentration field is approximately equal to the viscous cutoff scale (i.e., Kolmogorov scale) at which viscous dissipation becomes important in the velocity field.

Well-resolved single-point concentration measurements in the plume were obtained using a very fast-response photoionization detector (TIP-SJ2) that was specifically designed and developed for this purpose by S. & J. Engineering, Inc. (Richmond Hill, Ontario, Canada). The response time of the detector, obtained by measuring the rise time (5% to 95%) of the leading edge of a very narrow pulse of gas delivered to the sampling inlet with a swinging pendulum apparatus, was about 10^{-3} s. The effective detection cell length of the detector, normal to the flow, was about 1.7 mm (compared to a typical

Kolmogorov length of about 0.5 to 1 mm in the atmosphere depending on the prevailing conditions), giving the detector an exceptional temporal and spatial resolution for full-scale atmospheric field studies. The concentration signal from the detector was digitized in real time at a sampling frequency of 4000 Hz using a high-speed, high-resolution 16-bit analog-to-digital (A/D) input and output board and multiplexer (HSDAS 16 and SMUX 64, Analogic Inc.). The sampling time for the experiment was 35 min resulting in 8.4×10^6 points for the measured plume concentration time series.

Measurements of wind velocity and turbulence were made simultaneously with the tracer release using a three-axis sonic anemometer/thermometer (model RSWS-201/3A, Applied Technologies, Inc.) mounted at a height of 3 m, and turbulence statistics were calculated from the anemometer records of the wind velocity components. The mean wind speed, U, at 3-m height was 4.0 m s^{-1}. The root-mean-square (rms) value, σ, of the velocity fluctuations was 0.83 m s^{-1}, where $\sigma^2 \equiv (\sigma_u^2 + \sigma_v^2 + \sigma_w^2)/3$ and σ_u, σ_v, and σ_w are the standard deviations of wind velocity in the alongwind (x), crosswind (y), and vertical (z) directions, respectively. The experiment was conducted under near-neutral atmospheric stratification (e.g., the Monin–Obukhov length L_{mo} was -269 m). The friction velocity, u_*, calculated using the surface stress measured as the eddy correlation $\overline{u'w'}$ was 0.42 m s^{-1}. Here, the overbar is used to denote a time average over the sampling time of the experiment. The mean rate of dissipation of turbulence kinetic energy, $\bar{\epsilon}$, estimated from the spectrum of the alongwind velocity component, was 0.065 m^2 s^{-3}. The Kolmogorov microscale, η, calculated according to $\eta = (\nu^3/\bar{\epsilon})^{1/4}$, gave a value of 0.5 mm. The Taylor microscale, λ, defined to be the ratio of the rms of the velocity fluctuations to the rms of the

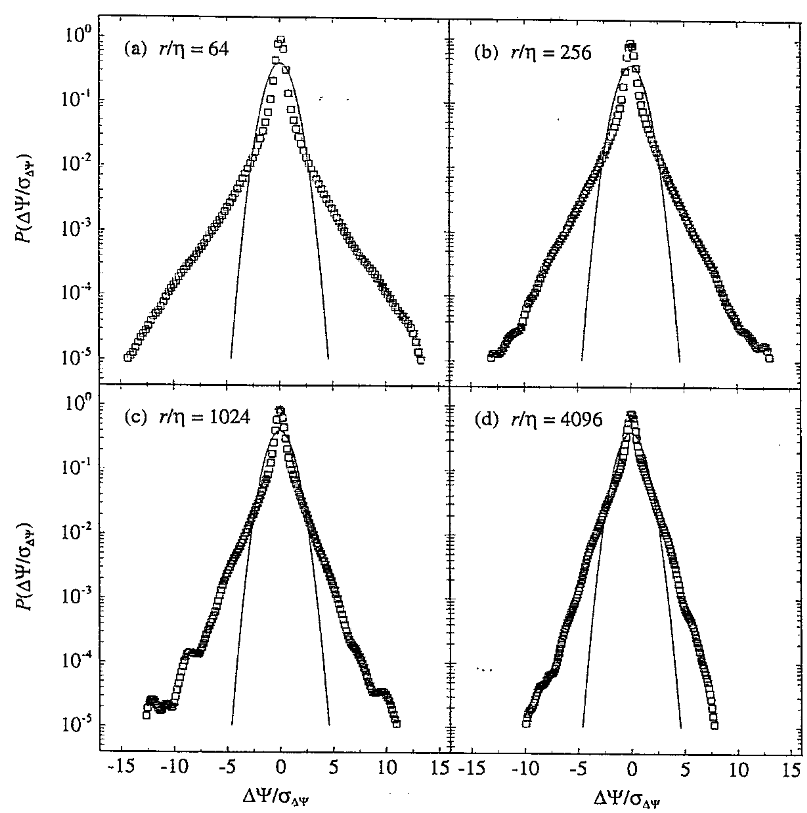

Fig. 1. The probability density function of the normalized concentration increments, $\Delta\Psi/\sigma_{\Delta\Psi}$, measured at four values of the normalized scale, r/η: (a)$r/\eta = 64$; (b)$r/\eta = 256$; (c)$r/\eta = 1024$; and, (d)$r/\eta = 4096$. A standard Gaussian distribution is included for comparison.

squared derivative of the velocity fluctuations, was found to be 9.4 cm. The Reynolds number R_λ, based on the Taylor microscale λ, was about 5200 for this experiment. Finally, the data examined here were from single-point concentration measurements in which Taylor's frozen turbulence hypothesis was invoked to relate temporal differences to spatial differences (i.e., the concentration increment $\Delta\Psi(r)$ at the separation distance r was obtained by taking the concentration increment over a time difference δt with $r = -U\delta t$). In this context, it should be noted that the estimation of the longitudinal (alongwind) scalar concentration derivative using Taylor's hypothesis has been experimentally and numerically validated by Antonia et al. [11] and Piomelli et al. [12] for turbulence intensity levels less than about 20 percent.

For the present high Reynolds number turbulent flow, the concentration power spectrum was found to exhibit a very extensive inertial-convective subrange having a power-law behavior with an exponent of about -1.65 ± 0.05 (close to the Obukhov–Corrsin scaling of $-5/3$) extending over about 2.5 decades of scaling of r/η from about 32 to 8000 [10]. We determined the PDF of concentration increments at a fixed scale r, for a range of different values of r that were logarithmically equally spaced, ranging from 4η to 800000η. Fig. 1 shows the semi-logarithmic plots of some typical examples of PDFs of the normalized concentration increment, $\Delta\Psi/\sigma_{\Delta\Psi}$, for four different values of the separation r in the inertial-convective subrange. Here, $\sigma_{\Delta\Psi}$ denotes the standard deviation of $\Delta\Psi$ at a fixed scale r. The standard Gaussian PDF has been included in the plots for comparison. Note that all the PDFs of $\Delta\Psi/\sigma_{\Delta\Psi}$ are very different from the Gaussian PDF. In particular, the PDFs of the concentration increments are leptokurtic in the sense that the tails of the PDFs are more strongly spread when compared with the Gaussian PDF, and this spreading of the tails progressively increases as r/η decreases throughout the inertial-convective subrange of scales. Interestingly, the PDFs of the concentration increments exhibit a departure from perfect symmetry, and this observation is consistent with the measured negative skewness in the increments (see below).

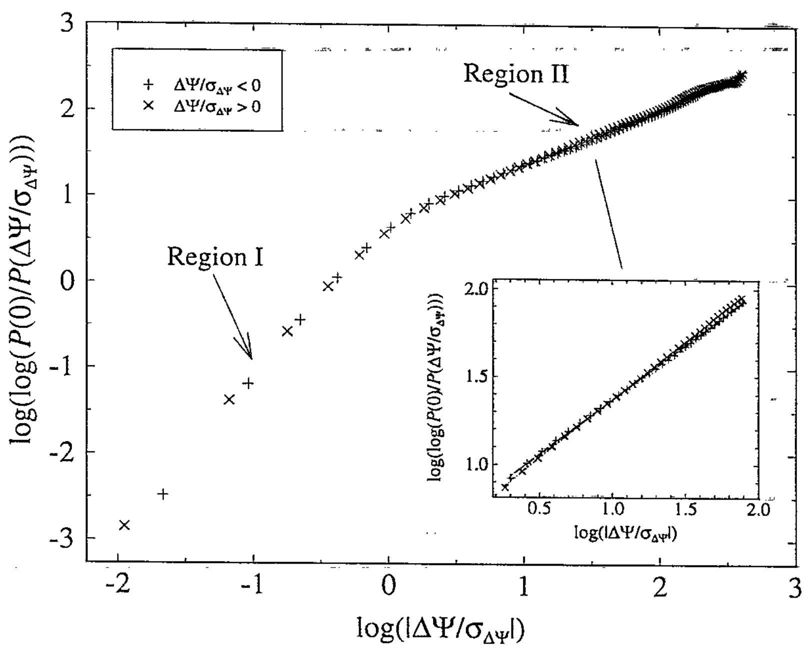

Fig. 2. A typical plot of $\log\{\log[P(0)/P(\Delta\Psi/\sigma_{\Delta\Psi})]\}$ versus $\log(|\Delta\Psi/\sigma_{\Delta\Psi}|)$ for both the negative and positive tails of the concentration increment PDF at the normalized scale $r/\eta = 256$. The tail slope $q(r)$ (stretching exponent) and the tail intercept $\kappa(r)$ (logarithmic decrement) are obtained by determining the slope and intercept, respectively, of the linear least-squares fit to the points in Region II (inset).

We now investigate quantitatively the tail behavior of the PDFs of $\Delta\Psi/\sigma_{\Delta\Psi}$ as a function of the scale r. To that end, we have fitted the PDF tails with a stretched exponential PDF with the form,

$$P(\Delta\Psi/\sigma_{\Delta\Psi}) = P(0)\exp\left(-\kappa(r)\,|\Delta\Psi/\sigma_{\Delta\Psi}|^{q(r)}\right), \qquad (1)$$

where $\kappa(r)$ is the logarithmic decrement and $q(r)$ is a "stretching" exponent that characterizes the extent of the tails of the PDF. We interpret q as a measure of the degree of intermittency of the underlying random process (viz., the smaller the value of q, the longer the PDF tail, and the more intermittent is the underlying process). Finally, note that the tails of the PDF in Eq. (1) depend critically on q. For $q = 2$, the PDF exhibits Gaussian tails; for any $q < 2$, the tails of the PDF are longer than those from a Gaussian PDF. In particular, for $q = 1$ the PDF has exponential tails.

The logarithmic decrement, $\kappa(r)$, and the stretching exponent, $q(r)$, can be determined by plotting $\log\{\log[P(0)/P(\Delta\Psi/\sigma_{\Delta\Psi})]\}$ versus $\log(|\Delta\Psi/\sigma_{\Delta\Psi}|)$. If the PDF tails are well represented by the stretched exponential form of Eq. (1), then a straight line with slope q and intercept κ will be obtained. A typical example of such a plot is exhibited in Fig. 2 for one value of separation distance r; namely, for $r/\eta = 256$. The example in Fig. 2 shows both the left- and right-side (i.e., the negative and positive) tails of the PDF. Note that each side of the PDF consists of two regions, each of which is associated with a particular linear régime. The central region of the PDF, correponding to values of $\Delta\Psi$ around zero, consists of an extruded peak (cf. Fig. 1). This pointed central region corresponds to Region I shown in Fig. 2. This region is restricted approximately to $|\Delta\Psi/\sigma_{\Delta\Psi}| \lesssim 1$ or, equivalently, to the region $\log(|\Delta\Psi/\sigma_{\Delta\Psi}|) \lesssim 0$. Region II of the PDF shown in Fig. 2 is rather extensive, and corresponds to the tails of the PDF. A very good straight-line fit can be obtained in the tail region, as shown in the inset of Fig. 2. The solid lines in the inset are least-squares fits to the data which show linear behavior, with typical coefficients of determination greater than about 0.99. This linear behavior implies that the stretched exponential form of Eq. (1) provides a very good model for the PDF tails.

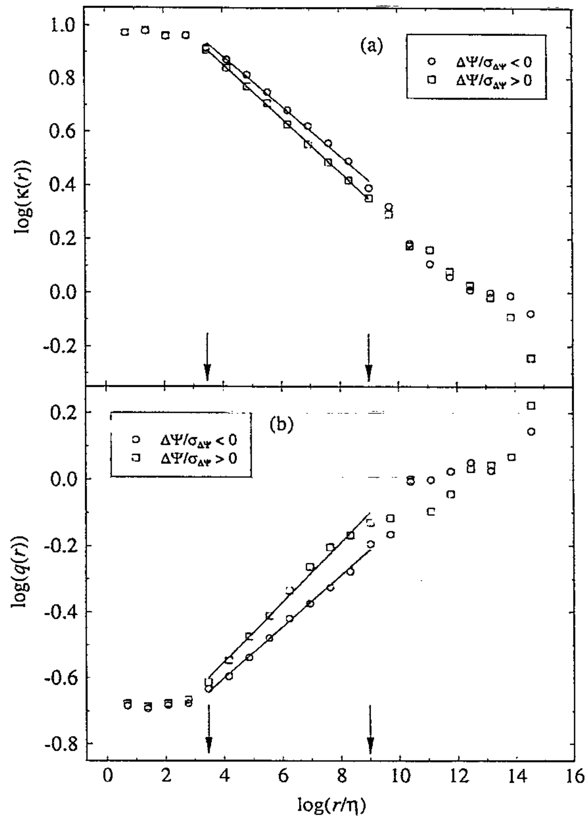

Fig. 3. The dependence of (a) the tail intercept κ (logarithmic decrement) and (b) the tail slope q (stretching exponent) on the normalized scale r/η, for both the negative and positive tails of the concentration increment PDF.

Fig. 3 shows the logarithmic increment (tail intercept), $\kappa(r)$, and the stretching exponent (tail slope), $q(r)$, plotted against the normalized separation distance r/η for both the negative and positive tails. Generally, there is an asymmetry in the negative and positive tails with the result that there are small differences between the behavior of κ and q for the two tails. Ignoring the small differences between the positive and negative tails for the moment, Fig. 3 shows that κ and q monotonically increases and decreases, respectively, with decreasing r within the inertial-convective subrange (with the bounds for this subrange delineated by the vertical arrows in Fig. 3). This behavior of κ and q with r is a characteristic expression of the internal intermittency of the scalar concentration fluctuations. Furthermore, the fact that neither κ nor q remains constant in the inertial-convective subrange implies that the PDF of concentration increments over this range of scales is not self-similar, and provides evidence (albeit indirect) for the multiscaling nature of plume concentrations in the inertial-convective subrange. The stretching exponent q continues to increase with increasing scales r/η larger than those associated with the inertial-convective subrange, up to a limiting value of 1, which corresponds to an exponential behavior for the PDF tails. Indeed, for the concentration increment over two widely separated points (i.e., large r), the concentrations at the two points become statistically independent of each other and the PDF of the concentration increments asymptotes to the PDF of the concentration itself. The PDF of the plume concentration fluctuations have been shown previously [5,10] to exhibit close to exponential behavior. Finally, data in Fig. 3 suggest that a reasonable fit to the functional dependence of κ and q on r within the inertial-convective subrange of scales can be obtained with a power-law of the form $\kappa(r) \sim r^{a}$ ($a < 0$) and $q(r) \sim r^{b}$ ($b > 0$). The power-law exponents a and b have been estimated separately from both the negative and positive PDF tails and yield the following results,

$$\begin{aligned} \kappa(r) &\sim r^{-0.093 \pm 0.003}, \quad \text{for } \Delta\Psi < 0, \\ &\sim r^{-0.101 \pm 0.001}, \quad \text{for } \Delta\Psi > 0, \end{aligned} \tag{2}$$

and

$$\begin{aligned} q(r) &\sim r^{0.078 \pm 0.002}, \quad \text{for } \Delta\Psi < 0, \\ &\sim r^{0.090 \pm 0.003}, \quad \text{for } \Delta\Psi > 0. \end{aligned} \tag{3}$$

The degree to which the small scales in a passively advected scalar are statistically isotropic is related to the magnitude of the skewness of the concentration increments,

$$S(r) = \frac{\langle (\Delta\Psi(r))^3 \rangle}{\sigma^3_{\Delta\Psi(r)}}.$$

The intermittency of the small-scale structures in the passive scalar concentration can be revealed by measuring the kurtosis of the concentration increments,

$$K(r) = \frac{\langle (\Delta\Psi(r))^4 \rangle}{\sigma^4_{\Delta\Psi(r)}}.$$

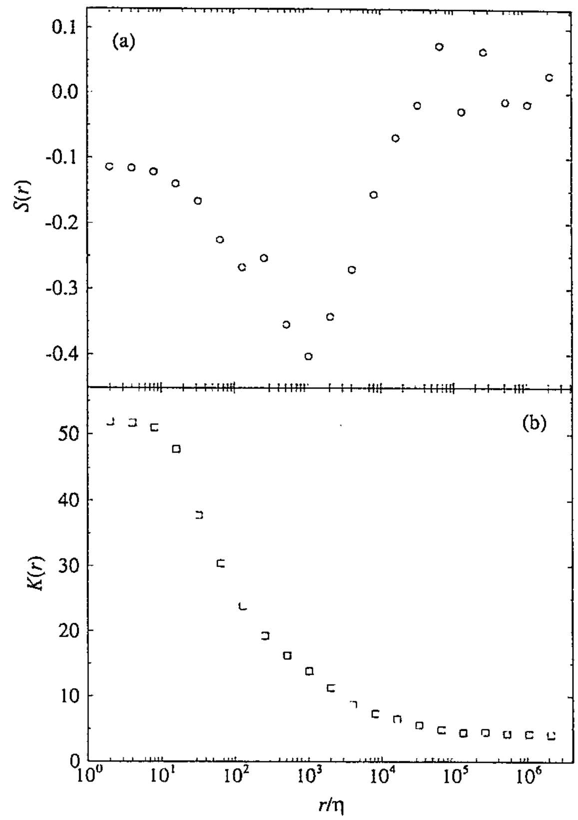

Fig. 4. The variation of (a) skewness S and (b) kurtosis K of the concentration increments with the normalized scale r/η.

The variation of $S(r)$ and $K(r)$ as a function of the separation distance r is shown in Fig. 4. It can be seen that S does not appear to vanish for scales within the inertial-convective subrange. Indeed, even at small scales within the inertial-convective subrange, S assumes a value from between about -0.4 to -0.2 with no apparent clear-cut trend in variation with r/η. It appears that the precise value for S in the inertial-convective subrange may depend on the characteristics of the large-scale mean flow and mean concentration field (e.g., mean shear and gradient in the mean concentration). On the other hand, $F(r)$ appears to increase monotonically with decreasing r/η in the inertial-convective subrange, approaching a limiting value of about 50 at the small-scale end of the inertial-convective subrange ($r/\eta \lesssim 32$). The increase of $F(r)$ with decreasing scales throughout the inertial-convective subrange is consistent with the notion that the PDF of concentration increments is not self-similar for scales within the inertial-convective subrange; and, in particular, the difference of concentration over the scale r becomes more and more intermittent (i.e., less and less space-filling) at smaller scales r, implying that their distribution exhibits progressively greater departures from a Gaussian distribution at smaller scales. This feature is consistent with the scale-dependent form of the PDF of $\Delta\Psi(r)$ just discussed.

The essential features of the PDF of concentration increments at different resolutions r become clearer when they are applied to determine the power-law scalings and scaling exponents of the concentration structure function. Because the PDF of $\Delta\Psi(r)$ is non-Gaussian and does not possess a self-similar form as a function of scale r (viz., either $\kappa(r)$ or $q(r)$ defined in Eq. (1) is not a constant in the inertial-convective subrange of scales), we expect an anomalous scaling of $\Delta\Psi(r)$. Specifically, the nth moment of the concentration increment $\Delta\Psi$ at scale r is used to define the scaling exponent ξ_n through

$$\langle |\Delta\Psi(r)|^n \rangle = \int_{-\infty}^{\infty} |\Delta\Psi(r)|^n P(\Delta\Psi(r);\, r)\, \mathrm{d}\Delta\Psi(r) \sim r^{\xi_n}, \tag{4}$$

where $P(\Delta\Psi(r);\, r)$ is the PDF of the concentration increments at resolution r. It has been demonstrated above that the tails of this PDF assume the form exhibited in Eq. (1) with the magnitude of the tail intercept $\kappa(r)$ being a decreasing power-law function of r and the tail slope $q(r)$ being an increasing power-law function of r summarized in Eqs. (2) and (3), respectively. This observed tail behavior can be used to increase the extent of the measured PDF $P(\Delta\Psi(r);\, r)$ and, hence, permit closure in the determination of the high-order moments of $\Delta\Psi$ (i.e., reliable measurement of high-order moments typically require sample sizes that increase exponentially with moment order n, with the result that the determination of ξ_n for large values of n may not be possible using the necessarily limited number of data samples available during any experimental procedure). To that end, the mathematical model for the PDF tails given by Eqs. (2) and (3) can be used to extrapolate the PDF to a very small probability level

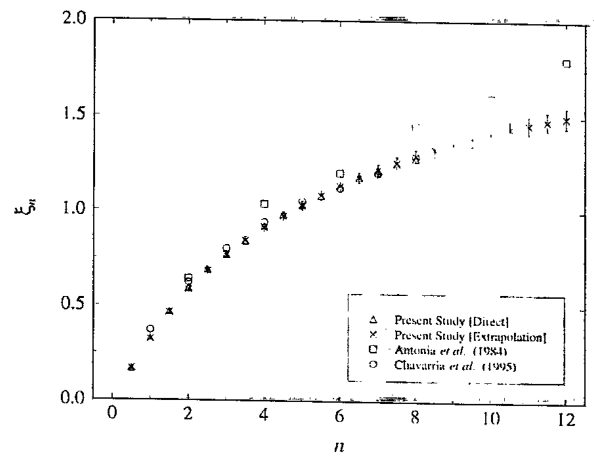

Fig. 5. Scaling exponents, ξ_n, of the concentration structure function plotted against the moment order n obtained in the present study, compared with measurements (in a fluctuating temperature field) obtained by Antonia et al. [9] and Chavarria et al. [13]. The scaling exponents for the present study have been determined using a direct method and an extrapolation procedure.

starting from the left-most and right-most points of the measured concentration increment PDF. These small probability levels correspond to the occurrence of rare events or rare instances of large concentration increments that cannot be probed by the detector in the fixed sampling time of the experiment. The moments of the concentration increments are readily evaluated by numerically integrating Eq. (4) using the measured PDF $P(\Delta\Psi(r);\, r)$ and including all points added to this PDF by extrapolation. This is repeated for 25 values of r logarithmically equally spaced in the inertial-convective subrange and for n-values ranging from 1 to 12 in incremental steps of 0.5. Generally, we found that the log-log plots of the concentration structure function exhibited a clear scaling region with a power-law behavior within the inertial-convective subrange spanning about 2 decades in scale. The slope of this power-law region then yields the local scaling exponents ξ_n for the concentration structure function.

Fig. 5 shows the measured concentration structure function exponents ξ_n plotted as a function of n. The comparison between the present scaling exponents and two other available measurements provided by Antonia et al. [9] (who measured temperature fluctuations on the centerline of a turbulent round jet) and Chavarria et al. [13] (who measured temperature fluctuations downstream of a heated mandoline in a wind tunnel) is also exhibited in Fig. 5. The scaling exponents determined in the present study were obtained using two methods: (1) a direct method that uses the least-squares fits to the high-order structure functions computed from the available data points; and (2) an extrapolation procedure that uses the stretched-exponential PDF model to extend the tails of the measured concentration increment PDF. The direct method was used to determine the scaling exponents for values of n up to 8; viz., it was determined that the data records were sufficiently long to ensure statistical convergence for values of n up to 8. We note that the scaling exponents obtained using the direct method and the extrapolation procedure agree within the overall experimental uncertainty. Furthermore, our values for ξ_n agree within experimental errors with the values reported by Chavarria et al. [12] for $n \leqslant 8$. However, our scaling exponents tend to fall below those obtained by Antonia et al. [9] for large n (and, particularly, for $n = 10$ and 12). It is important to note that in Antonia et al. [9], the scaling exponents for $n = 10$ and 12 were not measured directly. Rather, they were obtained by extrapolating the PDF of temperature increments in two different ways; namely, (1) by using an exponential tail in the PDF for the evaluation of temperature increment moments for $n \geqslant 10$, and (2) by applying successive approximations to the integrand (cf. Eq. (4)) $(\Delta\Psi(r))^n P(\Delta\Psi(r); r)$ starting with $n = 8$. It is clear that the scaling exponents ξ_n for large n will depend on the rate of exponential decay assumed in the extrapolation.

In any case, all the measurements clearly imply that $\xi_n < n/3$ for $n \gtrsim 3$ (viz., ξ_n exhibits a clear non-linear behavior with n that is at variance with the Obukhov–Corrsin scaling law which predicts a linear scaling behavior associated with the absence of intermittency). This anomalous scaling of ξ_n and the lack of a self-similar form for the concentration increment PDF for scales in the inertial-convective subrange is a strong indication of the multiscaling (and, hence, multifractality) in the scalar concentration field. Allowing for experimental uncertainty, the second-order power-law exponent (i.e., $\xi_2 = 0.58 \pm 0.02$) appears to be consistent with the observed scaling exponent of the power spectrum in the inertial-convective subrange (i.e., 1.65 ± 0.05). In either case, we note that the deviations from the $2/3$ exponent for $\langle |\Delta\Psi(r)|^2 \rangle$ for r in the inertial-convective subrange, or equivalently from the $5/3$ exponent for the power spectrum appear to be rather small and probably difficult to detect reliably. However, the manifestation of small-scale intermittency effects in the scalar field become more noticeable as n increases. The comparison of our current measurements of ξ_n with those provided by other investigators suggests that the scaling behavior of the turbulent concentration fluctuations is a rather robust phenomenon. Also, in spite of the fact the molecular diffusivity D of the scalar used in our experiments is approximately equal to the kinematic viscosity ν of air, the fluctuations of the concentration increment field, nevertheless, appears to be stronger than those of the velocity increment field (viz., the spatial distribution of the concentration increment field appears to be more singular than that of the velocity increment field). The latter observation follows by comparing the scaling exponents ξ_n for the concentration increment field summarized in Fig. 5 with those for the velocity increment field presented by Anselment et al. [14], or by comparing the tails of the concentration increment PDF summarized in Figs. 1 and 3 with those of the velocity increment PDF presented by Praskovsky and Oncley [15]. Finally, whereas various phenomenological models for small-scale intermittency exist [16–18], the explanation and prediction of this phenomenon based on the basic governing equations (e.g., the Navier–Stokes equation for the velocity field and the advection–diffusion equation for the concentration field) without any adjustable parameters still remains an unresolved problem.

We would like to thank C. Biltoft and J.F. Bowers of the Meterology and Modeling Division, U.S. Army Dugway Proving Ground for providing the meteorological support for these experiments.

References

[1] J.E. Fackrell and A.G. Robins, J. Fluid Mech. 117 (1982) 1.
[2] B.L. Sawford, Boundary-Layer Meteorol. 38 (1987) 209.
[3] N. Dinar, H. Kaplan and M. Kleiman, Boundary-Layer Meteorol. 45 (1988) 157.
[4] K.R. Mylne and P.J. Mason, Q.J.R. Meteorol. Soc. 117 (1991) 177.

[5] E. Yee, R. Chan, P.R. Kosteniuk, G.M. Chandler, C.A. Biltoft and J.F. Bowers, J. Appl. Meteorol. 33 (1994) 996.
[6] A.M. Obukhov, Izv. Akad. Nauk SSSR Geogr. Geofiz. 13 (1949) 58.
[7] S. Corrsin, J. Appl. Phys. 22 (1951) 469.
[8] A.N. Kolmogorov, Dokl. Akad. Nauk SSSR 30 (1941) 299.
[9] R.A. Antonia, E.J. Hopfinger, Y. Gagne and R. Anselmet, Phys. Rev. A 30 (1984) 2704.
[10] E. Yee, R. Chan, P.R. Kosteniuk, G.M. Chandler, C.A. Biltoft and J.F. Bowers, Boundary-Layer Meteorol. 76 (1995) 41.
[11] R.A. Antonia, L.W.B. Browne, D. Britz and A.J. Chambers, Phys. Fluids 27 (1984) 87.
[12] U. Piomelli, J.L. Balint and J.M. Wallace, Phys. Fluids A 1 (1989) 609.
[13] G.R. Chavarria, C. Baudet, and S. Ciliberto, Europhys. Lett 32 (1995) 319.
[14] F. Anselmet, Y. Gagne, E.J. Hopfinger and R.A. Antonia, J. Fluid Mech. 140 (1984) 63.
[15] A. Praskovsky and S. Oncley, Phys. Rev. Lett. 73 (1994) 3399.
[16] R. Benzi, G. Paladin, G. Parisi and A. Vulpiani, J. Phys. A Math. Gen. 17 (1984) 3521.
[17] Z.S. She and S.A. Orszag, Phys. Rev. Lett. 66 (1991) 1701.
[18] B.K. Shivamoggi, Physica A 221 (1995) 460.

PHYSICS LETTERS A

Instructions to Authors (short version)

(A more detailed version of these instructions is published in the preliminary pages to each volume.)

Submission of papers

Contributions in triplicate should be sent to the editor whose expertise covers the research reported and with whom the author can communicate efficiently. Editorial Board, addresses and primary interests are given on page 2 of the cover. In case of doubt, contributions can be submitted directly to the Publisher at the address below. However, it should be realized that such papers will have to be forwarded to one of the Editors, which will result in some delay.

Original material. By submitting a paper for publication in Physics Letters A the authors imply that the material has not been published previously nor has been submitted for publication elsewhere and that the authors have obtained the necessary authority for publication.

Refereeing. All contributions will be refereed. The Editors reserve the right to edit contributions, whenever necessary, and to refuse papers which in their opinion do not satisfy conditions as to standard or contents. Linguistic corrections not affecting the meaning will be carried out by the Publisher.

Types of contributions

The *length* of the papers is not formally limited, but expedient and compact formulation, appropriate to a letters journal, is expected. The Editor may require the removal of figures, lengthy introductions, derivations, descriptions of apparatus or speculations if these are not essential for the efficient and clear communication of important new results. An *abstract* of less than 50 words is required.

Manuscript preparation

All manuscripts should be written in good English. The paper copies of the text should be prepared with double line spacing and wide margins, on numbered sheets. See notes opposite on electronic versions of manuscripts.

Structure. Please adhere to the following order of presentation: Article title, Author(s), Affiliation(s), Abstract, PACS codes and keywords, Main text, Acknowledgements, Appendices, References, Figure captions, Tables.

Corresponding author. The name, complete postal address, telephone and fax numbers and the e-mail address of the corresponding author should be given on the first page of the manuscript.

Classification codes/keywords. Please supply one to four classification codes (PACS and/or MSC) and up to six keywords of your own choice that describe the content of your article in more detail.

References. References to other work should be consecutively numbered in the text using square brackets and listed by number in the Reference list. Please refer to the more detailed instructions for examples.

Illustrations

Illustrations should also be submitted in triplicate: one master set and two sets of copies. The *line drawings* in the master set should be original laser printer or plotter output or drawn in black india ink, with careful lettering, large enough (3–5 mm) to remain legible after reduction for printing. The *photographs* should be originals, with somewhat more contrast than is required in the printed version. They should be unmounted unless part of a composite figure. Any scale markers should be inserted on the photograph, not drawn below it.

Colour plates. Figures may be published in colour, if this is judged essential by the Editor. The Publisher and the author will each bear part of the extra costs involved. Further information is available from the Publisher.

After acceptance

Notification. You will be notified by the Editor of the journal of the acceptance of your article and invited to send an electronic version of the accepted text to the Publisher.

Copyright transfer. You will be asked to transfer the copyright of the article to the Publisher. This transfer will ensure the widest possible dissemination of information.

No proofs. In order to speed up publication, all proofreading will be done by the Publisher and proofs are *not* sent to the author(s).

Electronic manuscripts

The Publisher welcomes the receipt of an electronic version of your accepted manuscript (preferably encoded in LaTeX). If you have not already supplied the final, revised version of your article (on diskette) to the Journal Editor, you are requested herewith to send a file with the text of the accepted manuscript directly to the Publisher by e-mail or on diskette (allowed formats 3.5" or 5.25" MS-DOS, or 3.5" Macintosh) at the address given below. Please note that no deviations from the version accepted by the Editor of the journal are permissible without the prior and explicit approval by the Editor. Such changes should be clearly indicated on an accompanying printout of the file.

Author benefits

No page charges. Publishing in Physics Letters A is free.

Free offprints. The corresponding author will receive 50 offprints free of charge. An offprint order form will be supplied by the Publisher for ordering any additional paid offprints.

Discount. Contributors to Elsevier Science journals are entitled to a 30% discount on all Elsevier Science books.

Contents Alert. Physics Letters A is included in Elsevier's pre-publication service Contents Alert and CoDaS.

Further information (after acceptance)

Elsevier Science B.V., Physics Letters A
Issue Management Physics and Materials Science
P.O. Box 2759, 1000 CT Amsterdam
The Netherlands
Tel.: +31 20 4852638
Fax: + 31 20 4852319
E-mail: NHPDESKED@ELSEVIER.NL

Printed in The Netherlands

North-Holland, an imprint of Elsevier Science